ACS APPLIED MATERIALS & INTERFACES

Research Article

www.acsami.org

# Fabrication of Monodisperse Porous Zirconia Microspheres and Their Phosphorylation for Friedel–Crafts Alkylation of Indoles

Jie He,[†] Jiwei Chen,[†] Lianbing Ren,[†] Yong Wang,*[,†] Chao Teng,[†] Mei Hong,[†] Jing Zhao,*[,†,‡] and Biwang Jiang*[,†]

[†]Guangdong Key Laboratory of Nano-Micro Materials Research, Key Laboratory of Chemical Genomics, Shenzhen Graduate School of Peking University, Shenzhen 518055, People's Republic of China

[‡]Institute of Chemistry and Biomedical Sciences, State Key Laboratory of Pharmaceutical Biotechnology, School of Life Sciences, Nanjing University, Nanjing, 210093, China

Supporting Information

**ABSTRACT:** Monodisperse porous zirconia ($ZrO_2$) microspheres with nanocrystallized framework were fabricated by impregnation of porous polymer microspheres as a novel hard template with zirconia precursors followed by calcination to remove the template. Porous phosphorylated zirconia (PhZr) microspheres were prepared by further treating porous zirconia microspheres with phosphoric acid. The morphology, structure, and properties of these microspheres were studied by scanning electron microscopy (SEM), transmission electron microscopy (TEM), $N_2$ adsorption/desorption measurement, FT-IR, and X-ray powder diffraction. The as-prepared zirconia and phosphorylated zirconia microspheres showed uniform particle size and well-defined morphology. The phosphorylated zirconia microspheres served as highly active solid acid catalysts for Friedel–Crafts alkylation of indoles with chalcones and could be reused for 22 cycles with negligible loss of activity. In situ pyridine-adsorbed FT-IR analysis of the best performing PhZr microspheres suggested the presence of both Lewis and Brønsted acid sites, and the total acidity as measured by temperature-programmed desorption of ammonia ($NH_3$-TPD) was 328 $\mu$mol·g$^{-1}$.

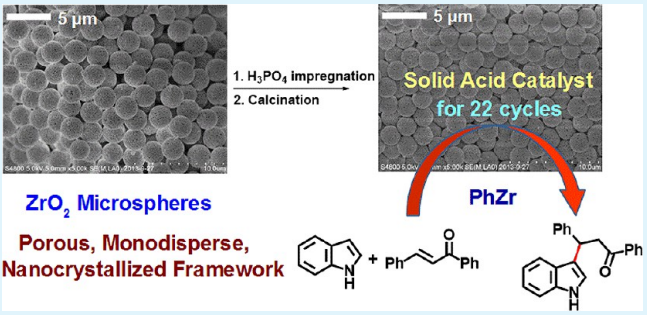


**KEYWORDS:** *monodisperse, porous zirconia microspheres, phosphorylation, Friedel–Crafts alkylation, indoles*

## 1. INTRODUCTION

Due to its excellent mechanical, electrical, optical, chemical, and thermal properties, zirconia has attracted widespread attention in various fields such as fuel cell,[1−3] adsorption,[4,5] chromatographic separation,[6−8] catalysis,[9−11] and sensors.[12−14] Controlling the morphology of zirconia materials during synthesis is of great importance, as the structural characteristics strongly determine the performance of zirconia.[15,16] For example, for application in chromatography separation, it is necessary to prepare porous zirconia microspheres with unique pore structure and narrow size distribution for high separation efficiency.[17] For use in catalysis, porous zirconia with large pores is required for ease of diffusion for large reacting molecules, and good crystalline zirconia nanoparticles account for high catalytic activity.[18,19] Therefore, it is essential to fabricate monodisperse porous zirconia microspheres with unique pore structure and nanocrystallized framework.

Porous zirconia microspheres have been fabricated by a few groups based on the polymerization-induced colloid aggregation (PICA) process,[20−22] oil emulsion method,[23] solvothermal process,[24] aerosol-assisted self-assembly approach,[25,26] and templating method.[27−29] McCormick et al. first prepared porous zirconia spheres using the PICA process and also combined the PICA process with an oil emulsion method to obtain hierarchically structured spherical particles.[22] However, the as-prepared porous zirconia microspheres had wide size distribution. Tsung et al. combined the acetic acid mediated sol–gel chemistry with the aerosol-assisted self-assembly approach to fabricate mesoporous zirconia submicrospheres with highly crystallized framework.[25] With et al. used spherical activated carbon as an exotemplate to synthesize hierarchically porous zirconia with irregular spherical morphology.[30] Despite their remarkable work on porous zirconia microspheres, it is still challenging to fabricate monodisperse micrometer-sized porous zirconia microspheres with nanocrystallized framework.

Recently, zirconia has found widespread applications in solid acid catalysis.[31−33] To form an efficient solid acid catalyst, zirconia is often modified by acid[34−37] or doped by other metals[38−42] (Fe, Co, Al, W). Modified zirconia has been widely employed in different reactions such as esterification, CO hydrogenation, Friedel–Crafts reaction, alkane isomerization, and dehydration of alcohol.[43−49] Zirconium oxophosphate/

Received: November 21, 2013
Accepted: January 21, 2014
Published: January 21, 2014

  

**Scheme 1. Fabrication of Monodisperse Porous Zirconia and Phosphorylated Zirconia Microspheres**

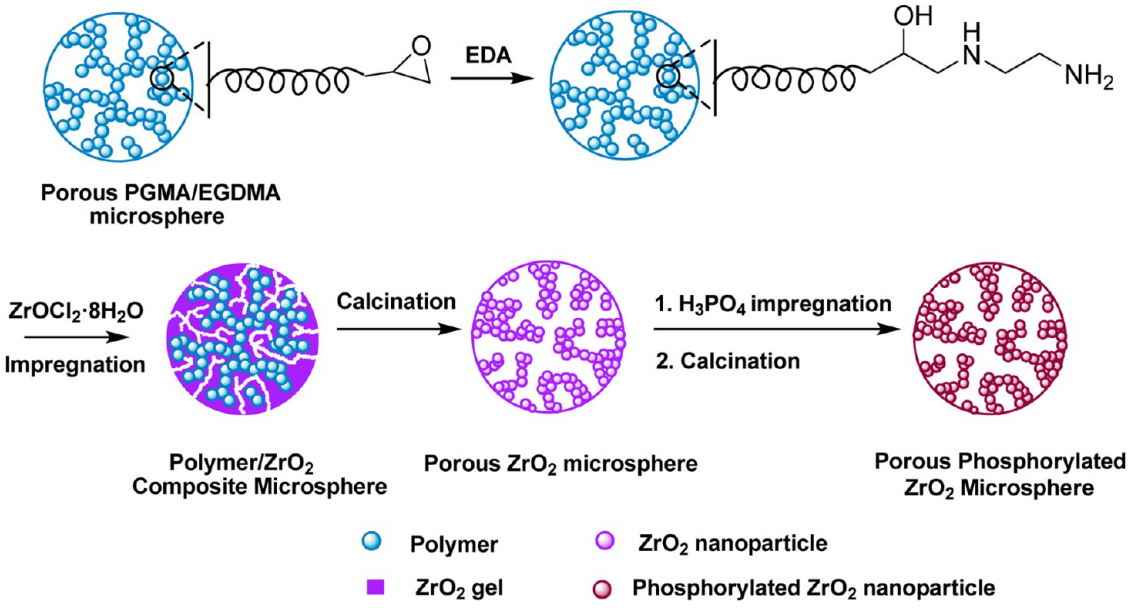


phosphate exhibits excellent catalytic efficiency in acid-catalyzed reactions.[50−52] Sinhamahapatra et al. fabricated mesoporous zirconium phosphate with worm-like pores and spherical morphology which can efficiently catalyze Friedel−Crafts benzylation of benzene to diphenylmethane.[52] However, these zirconium oxophosphate/phosphate materials possess an amorphous structure unless calcined at 900 °C. Compared with amorphous structure, nanocrystallized framework is a major area of interest because of its inherent large surface-to-volume ratio, quantum size effect, and unique catalytic performance.[53,54] Therefore, it is highly desirable to fabricate modified zirconia with nanocrystallized framework as a solid acid catalyst for various applications.

Herein we report an efficient and simple strategy to prepare monodisperse porous zirconia ($ZrO_2$) microspheres with nanocrystallized framework by applying porous polymer microspheres as a novel hard template. Phosphorylation of these porous zirconia microspheres for application in solid acid catalysis has been studied. $NH_3$-TPD and in situ FT-IR of pyridine-adsorbed analysis suggest the presence of tunable Lewis and Brønsted acidity of the phosphorylated zirconia (PhZr) microspheres, which has motivated us to develop their catalytic potential. The as-prepared PhZr microspheres exhibited excellent catalytic performance and recyclability for Friedel−Crafts alkylation of indoles with chalcones. The catalysts could be used at room temperature and reused for at least 22 cycles without loss of activity.

## 2. EXPERIMENTAL SECTION

**2.1. Chemicals and Materials.** The zirconia precursor zirconium oxychloride ($ZrOCl_2·8H_2O$) was purchased from Alfa Aesar. Ethylenediamine (EDA) was purchased from Sigma-Aldrich. The hard template porous polymer microsphere named poly(GMA-co-EGDMA) is a polymer of glycidyl methacrylate (GMA) cross-linked with ethylene glycol dimethacrylate (EGDMA) supplied by Nano-Micro Technology Company, China. Other substrates such as indole and chalcone used in the catalytic study of phosphorylated zirconia were all purchased from Sigma-Aldrich, and anhydrous solvents were distilled by standard procedure. Amberlyst-15 was purchased from Sigma-Aldrich. H-Beta zeolites were purchased from Novel Company, China. USY zeolite was supplied from Zouping Mingyuan Company, China. Water was purified by distillation followed by deionization using ion exchange resins. All chemicals were analytical grade and used without further purification.

**2.2. Preparation of $ZrO_2$ Microspheres.** Monodisperse porous zirconia microspheres were fabricated by impregnation of porous poly(GMA-co-EGDMA) microspheres with zirconia precursors followed by calcination to remove the template. In a typical synthesis, the poly(GMA-co-EGDMA) microspheres were first functionalized by EDA. Poly(GMA-co-EGDMA) microspheres of 10 g were dispersed in 240 mL of water and sonicated for 0.5 h before 10 g of EDA was added, and the mixture was mechanically stirred at 80 °C for 24 h. The resulting EDA-functionalized poly(GMA-co-EGDMA) microspheres were washed repeatedly with distilled water until the filtrate was neutral and dried at 50 °C. Afterwards, the EDA-functionalized poly(GMA-co-EGDMA) microspheres of 1 g were mixed with 2.5 g of $ZrOCl_2·8H_2O$, 4 mL of water, and 6 mL of ethanol. The mixture was then sonicated for 10 min and dried at 90 °C. Finally, the obtained poly(GMA-co-EGDMA)/zirconia composite microspheres were calcined at 600 °C for 6 h to form monodisperse porous zirconia microspheres.

**2.3. Preparation of PhZr Microspheres.** Porous phosphorylated zirconia microspheres were obtained by impregnating 0.3 g of porous zirconia microspheres with different amounts of 0.1 M $H_3PO_4$. The mixture was then dried at 100 °C followed by calcination at 600 °C for 3 h to form a phosphorylated porous zirconia microsphere denoted as PhZr-*X*. PhZr-1, 2, 3, 4, 5, and 6 (the mol ratio of Zr:P ≈ 1:0.082, 0.123, 0.144, 0.205, 0.699) mean that 0.3 g of zirconia microspheres was treated by 2, 3, 3.5, 4, 5, and 17 mL of 0.1 M $H_3PO_4$, respectively.

**2.4. Catalytic Study of PhZr Microspheres.** Friedel−Crafts alkylation of indoles with chalcones was carried out using porous phosphorylated zirconia microsphere as the catalyst. Before the reaction, the catalyst was evacuated at 100 °C for activation. In a typical synthesis, indole (0.2 mmol), chalcone (0.3 mmol), catalyst (0.2 g), and solvent (2 mL) were added to the flask. The reaction was conducted at room temperature. Thin-layer chromatography (TLC) was used to monitor the reaction. After the reaction was finished, the reaction mixture was centrifuged. The product was obtained by chromatography separation of the supernatant. The catalyst was then washed repeatedly with $CH_2Cl_2$ and dried at 50 °C followed by calcination at 600 °C for reuse.

**2.5. Characterization Techniques.** Powder X-ray diffraction (XRD) of zirconia microspheres was recorded using a Rigaku D/Max-2200PC diffractometer with Cu K$\alpha$ at 40 kV, 200 mA. The crystallite size determined by XRD was calculated using the Williamson−Hall

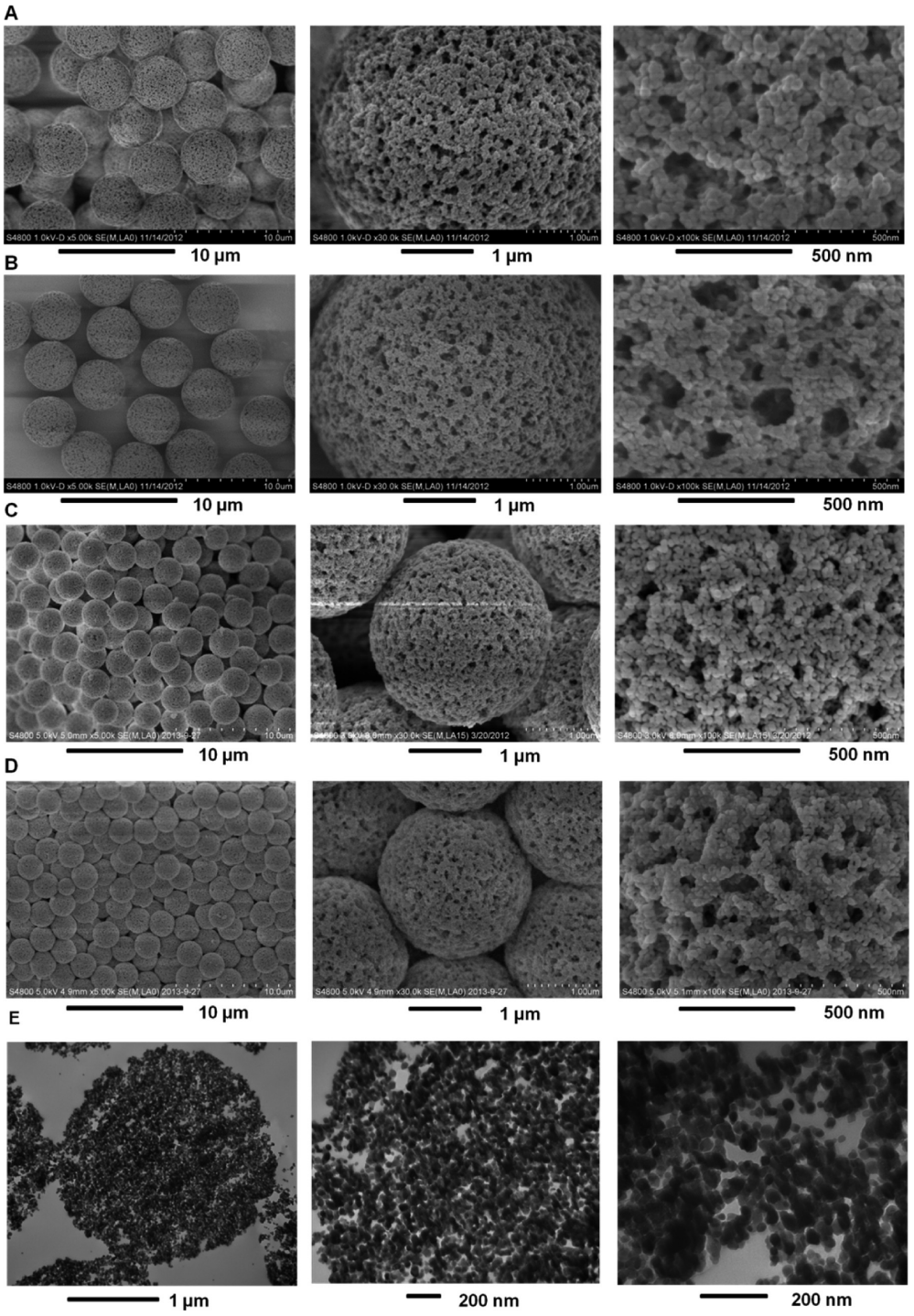


**Figure 1.** SEM images of (A) porous polymer microspheres, (B) porous polymer/zirconia composite microspheres, (C) porous zirconia microspheres, and (D) porous PhZr-3 microspheres. (E) TEM images of porous zirconia microspheres.

method. A field emission scanning electron microscope (SEM) Hitach S4800 was used for the determination of the morphology and structure of the microspheres. The particle hydrodynamic size was measured by using a Beckman Coulter Counter laser size analyzer (Multisizer 3). Transmission electron microscope images were collected on an FEI Tecnai G2 TEM. $N_2$ adsorption/desorption isotherms were measured at 77 K on a Micromeritics Tristar 3020. Thermogravimetric analysis (TGA) was performed on a Du Pont TGA 2050, with a heating rate of 10 °C $min^{-1}$. Fourier transform infrared (FT-IR) spectra of these samples were collected on a Shimadzu IR Prestige-21 with resolution of 4 $cm^{-1}$. In situ FT-IR of pyridine adsorbed on PhZr microspheres to characterize the acid sites and strength of the catalysts was conducted with a self-supported wafer of the sample using an EQUINOX 55 FT-IR spectrometer. The sample was first heated to 450 °C and kept for 1 h under vacuum. After cooling to room temperature, spectra of the unexposed sample were taken. Then the sample was exposed to pyridine and adsorbed for 3 min. The physically adsorbed pyridine was removed at 150 °C for 30 min under vacuum. Finally, the pyridine adsorbed infrared spectra were collected. Temperature-programmed desorption of ammonia ($NH_3$-TPD) was conducted to detect the total acidity of PhZr microspheres. $NH_3$-TPD was carried out from 120 °C to 600 °C with a heating rate of 10 °C $min^{-1}$ on Chemisorber AutoChem 2910. The samples were activated under the flow of He at 450 °C for 1 h

**Table 1. Properties of Template and As-Prepared Microspheres**

| microspheres | particle size (mean + SD) ($\mu$m) | BET surface area ($m^2 \cdot g^{-1}$) | pore volume ($cm^3 \cdot g^{-1}$) | acidity ($\mu mol \cdot g^{-1}$) |
|---|---|---|---|---|
| polymer | 4.74 ± 0.121 | 61 | 0.48 | - |
| polymer/$ZrO_2$ | 4.74 ± 0.135 | 0.85 | 0.02 | - |
| $ZrO_2$ | 2.56 ± 0.144 | 22 | 0.17 | 508 |
| PhZr-3 | 2.26 ± 0.137 | 5 | 0.06 | 328 |

followed by cooling to 120 °C, and ammonia adsorption was carried out at this temperature. The evolved ammonia was analyzed by online MS provided with a thermal conductivity detector (TCD). NMR spectra were recorded on a BrükerAvance-III 400 MHz instrument. Tetramethylsilane (TMS) served as an internal standard for NMR spectroscopy. EI high-resolution mass spectra were measured by an Elite Quadrupole time-of-flight mass spectrometer.

## 3. RESULTS AND DISCUSSION

**3.1. Preparation and Characterization of $ZrO_2$ and PhZr Microspheres.** As shown in Scheme 1, $ZrO_2$ microspheres were fabricated based on the hard-template method. In our previous reports, monodisperse porous silica and magnetic nanoparticle embedded silica microspheres have been successfully prepared using porous polymer microspheres as the hard template.[55,56] Porous poly(GMA-co-EGDMA) microspheres were chosen because of their surface epoxy groups and large pores. Porous poly(GMA-co-EGDMA) microspheres were first functionalized by ethylenediamine (EDA). The obtained EDA-functionalized poly(GMA-co-EGDMA) microspheres were then impregnated with $ZrOCl_2 \cdot 8H_2O$ in water/ethanol at 90 °C. During the impregnation and drying process, the zirconium precursors penetrated into the pore structure and incorporated into polymer microspheres with the aid of amino groups of the microspheres, and thus the sol−gel process occurred simultaneously. After drying, the composite microspheres were calcined at 600 °C to remove the polymer microspheres, and porous $ZrO_2$ microspheres were obtained. Secondly, PhZr microspheres were simply synthesized by treatment of a porous zirconia microsphere with 0.1 M $H_3PO_4$.

Figure 1A−C exhibits SEM images of polymer microspheres, zirconia/polymer composite microspheres, and porous zirconia microspheres. The zirconia/polymer composite microspheres show monodispersity similar to the original porous polymer microspheres without obvious size change, which indicates that the zirconium precursors entered into the pores and interacted closely with the polymer skeleton. The porous zirconia microspheres show well-defined morphology and excellent monodispersity and consist of spherical nanoparticles in the size range of about 15−50 nm. TEM images of porous zirconia microspheres in Figure 1E agree very well with the corresponding SEM images. A laser size analyzer was used to measure the sizes of the microspheres (Table 1). The particle sizes determined from the size analyzer are close to those measured from SEM images. The porous zirconia microspheres (about 2.56 $\mu$m) are much smaller than polymer microspheres due to shrinkage during calcination. The PhZr-3 microspheres (about 2.26 $\mu$m) are slightly smaller than that of $ZrO_2$ microspheres because of further shrinkage during calcination. It should be pointed out that PhZr-6 does not show well-defined spherical morphology, and the structure is destroyed by the excess phosphoric acid (Figure S1, Supporting Information).

The nitrogen adsorption/desorption results of the microspheres are shown in Figure 2 and Table 1. The template microspheres show a surface area of 61 $m^2 \cdot g^{-1}$ and pore volume

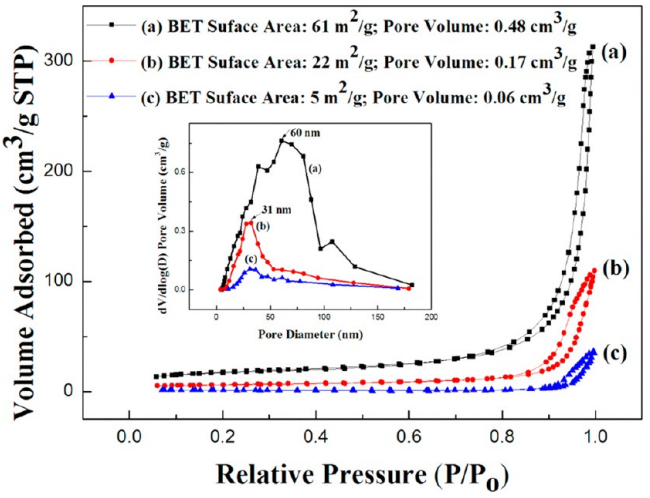


**Figure 2.** $N_2$ adsorption/desorption isotherms of (a) porous poly(GMA-co-EGDMA) microspheres, (b) porous $ZrO_2$ microspheres, and (c) porous PhZr-3 microspheres. The inset is pore diameter distribution of (a) porous poly(GMA-co-EGDMA) microspheres, (b) porous $ZrO_2$ microspheres, and (c) porous PhZr-3 microspheres.

of 0.48 $cm^3 \cdot g^{-1}$ with mainly macropores. After impregnation, the composite microspheres have very low surface area of only 0.85 $m^2 \cdot g^{-1}$ indicating that zirconia precursors entered into pores of the polymer microspheres successfully. Through calcination, the polymer part of the composite microspheres was removed to form porous zirconia microspheres. Porous zirconia contains mainly mesopores and exhibits a specific surface area of 22 $m^2 \cdot g^{-1}$ and pore volume of 0.17 $cm^3 \cdot g^{-1}$ with pore size of 31 nm. Compared with the template microspheres, the lower surface area and pore volume of porous zirconia microspheres are due to shrinkage of the skeleton, high density of zirconia, and growth of zirconia crystallite size during calcination. In contrast to porous $ZrO_2$ microspheres, PhZr-3 microspheres show lower surface area and pore volume but similar pore size owing to further crystallization of zirconia at high temperature.

The powder X-ray diffraction patterns for zirconia/polymer composite microspheres, porous zirconia microspheres, and porous PhZr-3 microspheres are shown in Figure 3. The zirconia/polymer composite microspheres show a broad peak indicating the amorphous structure of zirconia.[56] After calcination, X-ray diffraction patterns of porous zirconia microspheres exhibit many sharp peaks indicating good crystallinity. These peaks can be assigned to the tetragonal (JCPDS card no. 17-0923) and monoclinic (JCPDS card no. 37-1484) phase of $ZrO_2$. The average crystallite size was ca. 12 nm as calculated by the Williamson−Hall method suggesting nanocrystallized framework of porous zirconia microspheres. PhZr-3 microspheres retain these peaks in their wide-angle XRD. Additionally, peaks at 18.5°, 21.6°, 26.2°, and 36.1° appear, and they can be ascribed to crystalline zirconium

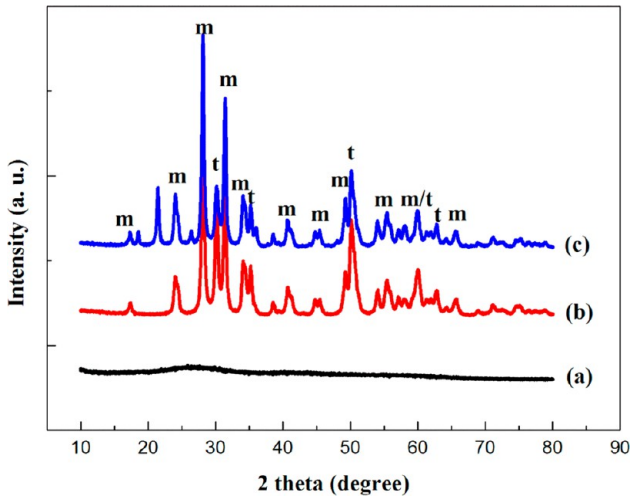


**Figure 3.** Wide-angle powder XRD patterns of (a) poly(GMA-co-EGDMA)/zirconia composite microspheres, (b) porous zirconia microspheres, and (c) PhZr-3 microspheres.

phosphate. Therefore, a part of crystallized zirconia was transformed to zirconium phosphate through treatment with phosphoric acid. With an excess amount of phosphoric acid, the obtained PhZr-6 microspheres show more crystalline zirconium phosphate (Figure S2, Supporting Information).

FT-IR spectra of the microspheres are exhibited in Figure 4. Through EDA functionalization of poly(GMA-co-EGDMA)

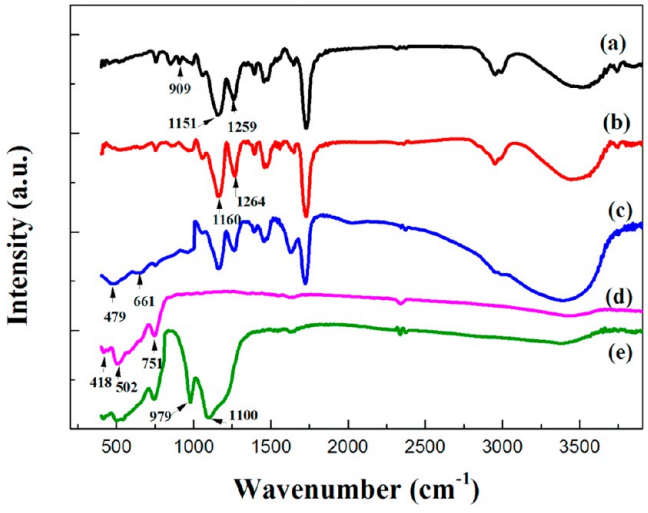


**Figure 4.** FT-IR spectra of (a) porous poly(GMA-co-EGDMA) microspheres, (b) EDA-functionalized poly(GMA-co-EGDMA) microspheres, (c) poly(GMA-co-EGDMA)/zirconia composite microspheres, (d) porous zirconia microspheres, and (e) PhZr-3 microspheres.

microspheres, the band at 909 $cm^{-1}$ of epoxide stretching vibration disappears, and the bands at 1151 and 1259 $cm^{-1}$ of epoxide characteristic peaks are transformed to 1160 and 1264 $cm^{-1}$ due to the formation of the C−N bond.[55] In contrast to EDA-functionalized poly(GMA-co-EGDMA) microspheres, the composite polymer/zirconia microspheres show obvious bands at 479 and 661 $cm^{-1}$ owing to the presence of Zr−O−Zr. The bands from polymer all disappeared in the IR spectra of porous zirconia microspheres indicating the removal of polymer through calcination. The bands between 418 and 751 $cm^{-1}$ suggest the formation of zirconia. For PhZr-3 microspheres, additional bands at 979 and 1100 $cm^{-1}$ are due to the P−O stretching vibrations indicating porous zirconia microspheres are successfully phosphorylated. The absence of phosphoryl peaks at 1300−1400 $cm^{-1}$ indicates the absence of $PO_4^{3-}$.[51]

As seen from thermogravimetric analysis (TGA) of the samples (Figure S3, Supporting Information), the polymer microspheres are completely burned away at 480 °C. For the polymer/zirconia composite microspheres, there are three stages of weight loss, 25−200, 200−550, and 550−700 °C. The weight loss below 200 °C is attributed to the gasification of small molecules such as adsorbed water of the microspheres due to incomplete drying. The weight loss between 200 and 500 °C is due to the decomposition/dehydration of the polymer chain and further condensation of zirconia in the polymer/zirconia composite microspheres. When the temperature is higher than 600 °C, the small and gradual weight loss (5.74 wt %) is attributed to further condensation of zirconia during crystallization and crystallite transformation.

**3.2. Catalytic Study of PhZr Microspheres.** PhZr microspheres can serve as a novel solid acid catalyst. Herein, Friedel−Crafts alkylation of indoles with chalcones is chosen as a model reaction to study the catalytic performance of PhZr microspheres. The catalytic efficiencies of $ZrO_2$ and PhZr-*X* microspheres are shown in Table 2, which were compared with

**Table 2. Friedel−Crafts Alkylation of Indoles with Chalcones Catalyzed by Porous PhZr Microspheres and Commercial Solid Acid Catalysts**[a]

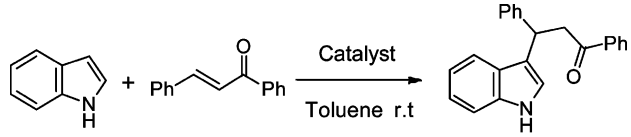


1 2 3

| entry | catalyst | *t*/h | isolated yield/% |
|---|---|---|---|
| 1 | $ZrO_2$ | 72 | trace |
| 2 | PhZr-1 | 16 | 55 |
| 3 | PhZr-2 | 16 | 86 |
| 4 | PhZr-3 | 6 | 98 |
| 5 | PhZr-4 | 16 | 73 |
| 6 | PhZr-5 | 16 | 43 |
| 7 | PhZr-6 | 72 | trace |
| 8[b] | USY | 16 | 72 |
| 9[c] | H-Beta | 16 | 46 |
| 10[d] | H-Beta | 16 | 35 |
| 11[e] | Amberlyst-15 | 16 | trace |

[a]Reaction conditions: catalysts: solid acid catalyst (0.2 g), indole (0.2 mmol), chalcone (0.3 mmol), toluene (2 mL). [b]USY Si/Al ratio at 5. [c]H-Beta Si/Al ratio at 40. [d]H-Beta Si/Al ratio at 100. [e]At rt, there was only a trace amount of product. At 80 °C, the yield achieved 21%.

those of some commercial solid acid catalysts in parallel. Porous zirconia microspheres could not catalyze the reaction. After treatment by phosphoric acid, the obtained PhZr microspheres exhibit good catalytic activities with high selectivity and no byproducts. PhZr-6 microspheres are ineffective because the structure is destroyed by excess phosphoric acid. Among PhZr-X microspheres, PhZr-3 microspheres show the best performance. The different catalytic performance of PhZr microspheres may be mainly related to their acidic properties. The PhZr-3 microspheres are also more superior to the commercial solid


dx.doi.org/10.1021/am405202d | ACS Appl. Mater. Interfaces 2014, 6, 2718−2725

acid catalysts of USY, H-Beta zeolite, and Amberlyst-15. A minimal loading of PhZr-3 microspheres for Friedel–Crafts alkylation of indoles with chalcones at elevated temperature was studied (Table S1, Supporting Information). The minimal loading to achieve 98% yield decreased almost an order of magnitude when the reaction temperature increased from room temperature to 110 °C. Solvent screening and substrate scope of different substituents on indoles and chalcones are shown in the Supporting Information (Table S2, Table S3, Supporting Information). The reaction could tolerate a wide range of substitution. Furthermore, compounds (4a–4d) were synthesized using PhZr-3 as the solid acid catalyst (Figure 5). The

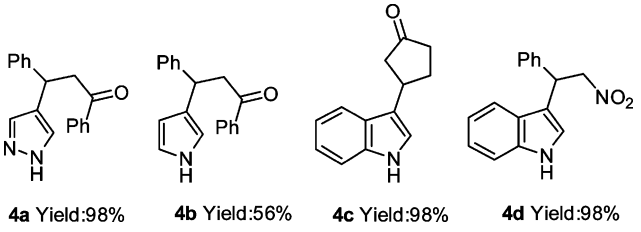


**Figure 5.** Further substrate scope of Friedel–Crafts alkylation catalyzed by PhZr-3.

reusability of PhZr-3 catalyst for Friedel–Crafts alkylation of indoles with chalcones was evaluated. After each run, the catalyst was calcined at 600 °C for activation. As shown in Figure 6, the PhZr-3 catalyst exhibited consistent high activity

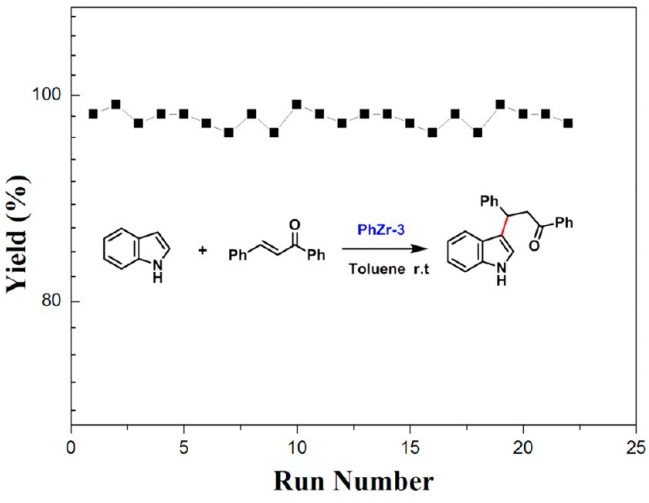


**Figure 6.** Reusability of PhZr-3 for Friedel–Crafts reaction of indoles and chalcones.

even after 22 recycles. Activation at lower temperatures was evaluated (Table S4, Supporting Information). It was essential for the used PhZr-3 catalyst to be activated at 600 °C for achieving 98% yield, which might be due to organics adsorbed on the acid sites and their incomplete removal at lower temperatures.

**3.3. Acidity Study.** In situ FT-IR of pyridine-adsorbed and temperature-programmed desorption of ammonia ($NH_3$-TPD) on the samples were explored to study the acidic properties of $ZrO_2$ and PhZr-*X* microspheres. Results of in situ FT-IR of pyridine adsorbed on the microspheres are shown in Figure 7. The bands at 1445 and 1607 $cm^{-1}$ are ascribed to the adsorption of pyridine on the Lewis acid sites, while the band at

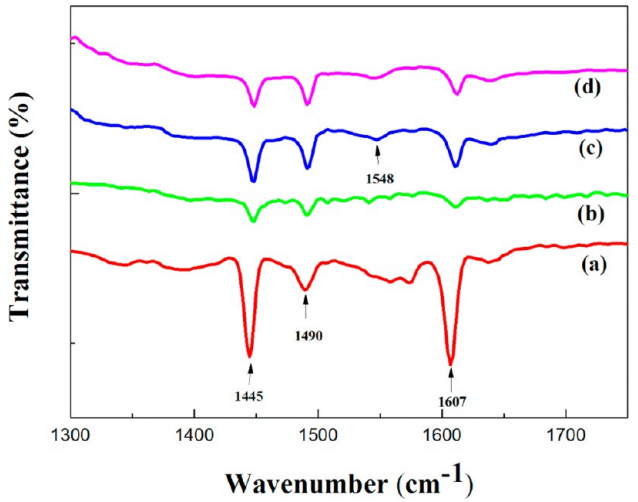


**Figure 7.** In situ FT-IR spectra of pyridine adsorbed on (a) $ZrO_2$, (b) PhZr-1, (c) PhZr-3, and (d) PhZr-4.

1548 $cm^{-1}$ is assigned to the Brønsted acid sites. The band at 1490 $cm^{-1}$ is due to the simultaneous adsorption of pyridine on both Brønsted and Lewis acid sites.[52] Porous zirconia microspheres exhibit strong Lewis acidity and poor Brønsted acidity. Treated by phosphoric acid, the obtained PhZr microspheres show lower Lewis acidity and appearing Brønsted acidity. Interestingly, by varying the amount of phosphoric acid, PhZr microspheres with different acidities are obtained, which play an important role in catalytic performance. $NH_3$-TPD has been carried out to measure the total acid amount of the samples (Table 1, Table S5, Supporting Information). PhZr-3 microspheres show one broad peak centered at 437 °C and strong acidity of 328 $\mu mol \cdot g^{-1}$.

## 4. CONCLUSION

We have fabricated monodisperse porous zirconia microspheres by impregnation of porous polymer microspheres with zirconia precursors followed by calcination to remove polymer microspheres. The obtained porous zirconia microspheres are monodisperse and micrometer-sized. Moreover, they exhibit nanocrystallized framework and well-defined spherical morphology with pore size at 31 nm and large pore volume of 0.17 $cm^3 \cdot g^{-1}$. Treated with phosphoric acid, the obtained porous PhZr microspheres serve as a novel solid acid catalyst and exhibit controlled acidities. The best PhZr microspheres surpassed common commercial solid acid catalysts such as USY, H-Beta zeolite, and Amberlyst-15 when catalyzing Friedel–Crafts alkylation of indoles with chalcones. The monodisperse porous phosphorylated zirconia microspheres are easily recyclable and could withstand over 22 cycles with almost no loss of catalytic activity. In all, we have developed a method to prepare monodisperse porous zirconia microspheres and phosphorylated zirconia microspheres with controlled acidities for Friedel–Crafts alkylation of indoles with chalcones. The strategy here may be applied to the design and preparation of more inorganic materials and functionalized materials for organic synthesis. The investigation on wider applications of monodisperse porous zirconia microspheres is still underway.

## ■ ASSOCIATED CONTENT

### Supporting Information

SEM image, XRD, TGA curves, $NH_3$-TPD curve, acidities, surface area, and pore volume of the samples, reusability experiments, a minimal loading of catalysts at elevated temperature, solvent screening, substrate scope, and NMR data for compounds (3a−3j and 4a−4d) have been given. This material is available free of charge via the Internet at http://pubs.acs.org.

## ■ AUTHOR INFORMATION


### Corresponding Authors

*E-mail: jiangbw@pkusz.edu.cn.
*E-mail: jingzhao@pkusz.edu.cn.
*E-mail: ywang@pkusz.edu.cn.


### Author Contributions

The manuscript was written through contributions of all authors. All authors have given approval to the final version of the manuscript.

### Notes

The authors declare no competing financial interest.

## ■ ACKNOWLEDGMENTS

This work is financially supported by grants of the National Basic Research Program of China (2010CB923303 to J.Z.). B.W.J. thanks the Shenzhen government (ZDSY20120614145053326). J.Z. thanks the Shenzhen Government (JC201104210113A and SW201110018), Guangdong Government (S20120011226), and the Fok Ying-Tong Education Foundation, China (132011 to J.Z.). Y.W. thanks the Shenzhen government (JCYJ201206141509581, JCYJ20130329181034621, JCYJ20120614151035045 and CXZZ20130322142615483).

## ■ REFERENCES


(1) Mamak, M.; Coombs, N.; Ozin, G. *J. Am. Chem. Soc.* **2000**, *122*, 8932−8939.
(2) Mamak, M.; Coombs, N.; Ozin, G. *Adv. Mater.* **2000**, *12*, 198−202.
(3) Shim, J. H.; Chao, C. C.; Huang, H.; Prinz, F. B. *Chem. Mater.* **2007**, *19*, 3850−3854.
(4) Xu, L.; Lee, H. K. *Anal. Chem.* **2007**, *79*, 5241−5248.
(5) Xu, S.; Whitin, J. C.; Yu, T. S.; Zhou, H.; Sun, D.; Sue, H. J.; Zou, H.; Cohen, H. J.; Zare, R. N. *Anal. Chem.* **2008**, *80*, 5542−5549.
(6) Dong, M. M.; Ye, M. L.; Cheng, K.; Song, C. X.; Pan, Y. B.; Wang, C. L.; Bian, Y. Y.; Zou, H. F. *J. Proteome Res.* **2012**, *11*, 4673−4681.
(7) Fields, S. M.; Ye, C. Q.; Zhang, D. D.; Branch, B. R.; Zhang, X. J.; Okafo, N. *J. Chromatogr. A* **2001**, *913*, 197−204.
(8) Jackson, P. T.; Carr, P. W. *J. Chromatogr. A* **2002**, *958*, 121−129.
(9) Miller, T. M.; Grassian, V. H. *J. Am. Chem. Soc.* **1995**, *117*, 10969−10975.
(10) Rulkens, R.; Tilley, T. D. *J. Am. Chem. Soc.* **1998**, *120*, 9959−9960.
(11) Steiner, S. A.; Baumann, T. F.; Bayer, B. C.; Blume, R.; Worsley, M. A.; MoberlyChan, W. J.; Shaw, E. L.; Schlögl, R.; Hart, A. J.; Hofmann, S.; Wardle, B. L. *J. Am. Chem. Soc.* **2009**, *131*, 12144−12154.
(12) Liu, G.; Lin, Y. *Anal. Chem.* **2005**, *77*, 5894−5901.
(13) Lu, D.; Wang, J.; Wang, L.; Du, D.; Timchalk, C.; Barry, R.; Lin, Y. *Adv. Funct. Mater.* **2011**, *21*, 4371−4378.
(14) Zhou, M.; Ahmad, A. *Mater. Res. Bull.* **2006**, *41*, 690−696.
(15) Stichert, W.; Schüth, F.; Kuba, S.; Knozinger, H. *J. Catal.* **2001**, *198*, 277−285.
(16) Arnal, P. M.; Weidenthaler, C.; Schüth, F. *Chem. Mater.* **2006**, *18*, 2733−2739.
(17) Clausen, A. M.; Carr, P. W. *Anal. Chem.* **1998**, *70*, 378−385.
(18) Liu, R.; Wang, X.; Zhao, X.; Feng, P. *Carbon* **2008**, *46*, 1664−1669.
(19) Jones, C. W.; Tsuji, K.; Davis, M. E. *Nature* **1998**, *393*, 52−54.
(20) Sun, L.; Annen, M. J.; Lorenzano-Porras, F.; Carr, P. W.; McCormick, A. V. *J. Colloid Interface Sci.* **1994**, *163*, 464−473.
(21) Annen, M. J.; Kizhappali, R.; Carr, P. W.; McCormick, A. V. *J. Mater. Sci.* **1994**, *29*, 6123−6130.
(22) Sathyagal, A. N.; Carr, P. W.; McCormick, A. V. *J. Colloid Interface Sci.* **1999**, *219*, 20−30.
(23) Trüdinger, U.; Müller, G.; Unger, K. K. *J. Chromatogr. A* **1990**, *535*, 111−125.
(24) Chen, D.; Cao, L.; Hanley, T. L.; Caruso, R. A. *Adv. Funct. Mater.* **2012**, *22*, 1966−1971.
(25) Tsung, C.-K.; Fan, J.; Zheng, N.; Shi, Q.; Forman, A. J.; Wang, J.; Stucky, G. D. *Angew. Chem., Int. Ed.* **2008**, *47*, 8682−8686.
(26) Grosso, D.; Soler Illia, G. J. de A. A.; Grepaldi, E. L.; Charleux, B.; Sanchez, C. *Adv. Funct. Mater.* **2003**, *13*, 37−42.
(27) Mouaziz, H.; Lacki, K.; Larsson, A.; Sherrington, D. C. *J. Mater. Chem.* **2004**, *14*, 2421−2424.
(28) Jin, Z.; Wang, F.; Wang, F.; Wang, J.; Yu, J. C.; Wang, J. *Adv. Funct. Mater.* **2013**, *23*, 2137−2144.
(29) Fan, X.; Song, X.; Yang, X.; Hou, L. *Mater. Res. Bull.* **2011**, *46*, 1315−1319.
(30) With, P.; Heinrich, A.; Lutecki, M.; Fichtner, S.; Böhringer, B.; Gläser, R. *Chem. Eng. Technol.* **2010**, *33*, 1712−1716.
(31) Kiss, A. A.; Dimian, A. C.; Rothenberg, G. *Adv. Synth. Catal.* **2006**, *348*, 75−81.
(32) Pandey, A. D.; Güttel, R.; Leoni, M.; Schüth, F.; Weidenthaler, C. *J. Phys. Chem. C* **2010**, *114*, 19386−19394.
(33) Sun, J.; Zhu, K.; Gao, F.; Wang, C.; Liu, J.; Peden, C. H. F.; Wang, Y. *J. Am. Chem. Soc.* **2011**, *133*, 11096−11099.
(34) Das, S. K.; Bhunia, M. K.; Sinha, A. K.; Bhaumik, A. *J. Phys. Chem. C* **2009**, *113*, 8918−8923.
(35) Kleitz, F.; Thomson, S. J.; Liu, Z.; Terasaki, O.; Schüth, F. *Chem. Mater.* **2002**, *14*, 4134−4144.
(36) Sun, Y.; Ma, S.; Du, Y.; Yuan, L.; Wang, S.; Yang, J.; Deng, F.; Xiao, F.-S. *J. Phys. Chem. B* **2005**, *109*, 2567−2572.
(37) Tabora, J. E.; Davis, R. J. *J. Am. Chem. Soc.* **1996**, *118*, 12240−12241.
(38) Drago, R. S.; Kob, N. *J. Phys. Chem. B* **1997**, *101*, 3360−3364.
(39) Hwang, C.-C.; Mou, C.-Y. *J. Phys. Chem. C* **2009**, *113*, 5212−5221.
(40) Kuba, S.; Gates, B. C.; Grasselli, R. K.; Knozinger, H. *Chem. Commun.* **2001**, 321−322.
(41) López, D. E.; Suwannakarn, K.; Bruce, D. A.; Goodwin, J. G., Jr. *J. Catal.* **2007**, *247*, 43−50.
(42) Shiju, N. R.; AnilKumar, M.; Hoelderich, W. F.; Brown, D. R. *J. Phys. Chem. C* **2009**, *113*, 7735−7742.
(43) Chen, X.-R.; Ju, Y.-H.; Mou, C.-Y. *J. Phys. Chem. C* **2007**, *111*, 18731−18737.
(44) Li, Z.; Wnetrzak, R.; Kwapinski, W.; Leahy, J. J. *ACS Appl. Mater. Interfaces* **2012**, *4*, 4499−4505.
(45) Yadav, G. D.; Pujari, A. A. *Green Chem.* **1999**, *1*, 69−74.
(46) Li, W.; Deng, Y.; Wu, Z.; Qian, X.; Yang, J.; Wang, Y.; Gu, D.; Zhang, F.; Tu, B.; Zhao, D. *J. Am. Chem. Soc.* **2011**, *133*, 15830−15833.
(47) Ferino, I.; Casula, M. F.; Corrias, A.; Cutrufello, M. G.; Monaci, R.; Paschina, G. *Phys. Chem. Chem. Phys.* **2000**, *2*, 1847−1854.
(48) Sohn, J. R.; Kim, J.-G.; Kwon, T.-D.; Park, E. H. *Langmuir* **2002**, *18*, 1666−1673.
(49) Chai, S. H.; Wang, H. P.; Liang, Y.; Xu, B. Q. *Green Chem.* **2008**, *10*, 1087−1093.
(50) Rao, K. N.; Sridhar, A.; Lee, A. F.; Tavener, S. J.; Young, N. A.; Wilson, K. *Green Chem.* **2006**, *8*, 790−797.
(51) Sinhamahapatra, A.; Sutradhar, N.; Roy, B.; Tarafdar, A.; Bajaj, H. C.; Panda, A. B. *Appl. Catal., A* **2010**, *385*, 22−30.

(52) Das, S. K.; Bhunia, M. K.; Sinha, A. K.; Bhaumik, A. *ACS Catal.* **2011**, *1*, 493−501.
(53) Das, S. K.; Bhunia, M. K.; Sinha, A. K.; Bhaumik, A. *J. Phys. Chem. C* **2009**, *113*, 8918−8923.
(54) Chen, H.; Gu, J.; Shi, J.; Liu, Z.; Gao, J.; Ruan, M.; Yan, D. *Adv. Mater.* **2005**, *17*, 2010−2014.
(55) He, J.; Yang, C.; Xiong, X.; Jiang, B. *J. Polym. Sci., Part A: Polym. Chem.* **2012**, *50*, 2889−2897.
(56) Wang, Y.; He, J.; Chen, J.; Ren, L.; Jiang, B.; Zhao, J. *ACS Appl. Mater. Interfaces* **2012**, *4*, 2735−2742.